

C-HCR assembly of branched DNA nanostructures for amplified uracil–DNA glycosylase assay

*Jing Wang, Min Pan, Jie Wei, Xiaoqing Liu, Fuan Wang**

Key Laboratory of Analytical Chemistry for Biology and Medicine (Ministry of Education),
College of Chemistry and Molecular Sciences, Wuhan University, Wuhan, P. R. China

* To whom correspondence should be addressed. E-mail: fuanwang@whu.edu.cn.

Table of Contents

Experimental SectionS-2

Figure S1. Construction of upstream hybridization chain reaction (HCR-1) circuitS-5

Figure S2. Construction of downstream hybridization chain reaction (HCR-2) circuitS-6

Figure S3. Optimization of the C-HCR system.....S-7

Figure S4. Demonstration of C-HCR strategyS-9

Figure S5. Gel electrophoresis characterization of C-HCR systemS-10

Figure S6. AFM investigation of C-HCR circuitS-11

Figure S7. Investigation of the specific UDG-substrate interactions.....S-12

Figure S8. Optimizaition of UDG recognition probeS-13

Figure S9. Optimization of UDG-involved reaction conditionsS-14

Figure S10. Traditional HCR-1-mediated UDG assayS-15

Figure S11. The kinetics analysis of the specific UDG-substrate interactionsS-16

Table S1. The DNA sequences used to construct the amplified sensing platformS-17

Table S2. Summary of the present amplification methods for UDG assayS-18

ReferenceS-19

Supporting Information

Experimental Section

Materials and apparatus

All oligonucleotides were synthesized, HPLC-purified and freeze-dried by Sangon Biotechnology Co., Ltd. (Shanghai, China). They were used as provided and diluted in phosphate buffer (20 mM, pH 7.0) to give stock solutions of 100 μM . The sequences of all oligonucleotides are listed in **Table S1**. Uracil–DNA-glycosylase (UDG), human Alkyladenine DNA Glycosylase (hAAG) were purchased from New England Biolabs (Ipswich, MA, USA). Sodium chloride, magnesium chloride, 4-(2-hydroxyethyl) piperazine-1 ethanesulfonic acid sodium salt (HEPES), 5-Fluorouracil (5-FU) and bovine serum albumin (BSA) were obtained from Sigma-Aldrich (MO, USA). All stock solutions of nucleic acids and enzymes were stored at $-20\text{ }^{\circ}\text{C}$ before use. Gentamycin was purchased from Aladdin Chemistry Co., Ltd. (Shanghai, China). GelRed was purchased from Biotium (CA, USA). All solutions were prepared by using ultrapure water, which was obtained through a Millipore Milli-Q water purification system with an electric resistance $>18.2\text{ M}\Omega\cdot\text{cm}$. Atomic force microscope (AFM) cantilever (SCANASYST-AIR) was purchased from Bruker (Camarilla, CA).

Fluorescence assay

For C-HCR execution, all hairpin probes (4 μM) were respectively heated to $95\text{ }^{\circ}\text{C}$ for 5 min, then cooled down rapidly and kept steadily at $25\text{ }^{\circ}\text{C}$ for at least 2 h before use. Unless specified, 50 nM of intact or UDG-treated initiator probe was introduced into the metastable mixture containing 200 nM H_1 , 100 nM H_2 , 200 nM H_3 , 200 nM H_4 , 100 nM H_5 , 200 nM H_6 to trigger the isothermal autonomous C-HCR process in reaction buffer (10 mM HEPES, 1 M NaCl, 50 mM MgCl_2 , pH 7.2) at room temperature ($25\text{ }^{\circ}\text{C}$). All fluorescence measurements were performed using a Cary Eclipse Device (Varian Inc.). The emission spectra were acquired by exciting the samples at 490 nm, and the fluorescence spectra were collected from 505 to 650 nm. The kinetically monitoring the fluorescence intensity changes were recorded at a fixed wavelength of 520 nm upon exciting the system at $\lambda = 490\text{ nm}$.

UDG detection and inhibitor screening

For detecting UDG, the UDG reaction mixture consisting of different amounts of UDG and 10 μM recognition probe was reacted in UDG incubation buffer (20 mM Tris-HCl, 1 mM DTT, 1 mM EDTA, pH 8) at $37\text{ }^{\circ}\text{C}$ for 15 min. To achieve the best performance, the incubation time and temperature of UDG reaction were optimized. 1 μL of each UDG-treated probe was transferred to 199 μL C-HCR mixture containing 200 nM H_1 , 100 nM H_2 , 200 nM H_3 , 200 nM H_4 , 100 nM H_5 , 200 nM H_6 to trigger the autonomous self-assembly process that was monitored by fluorescence measurement. Control experiments were carried out under the same conditions with interfering proteins (BSA or hAAG) or without UDG enzyme to investigate the selectivity of the C-HCR-amplified UDG assay. The concentrations of UDG, hoGG1 and BSA correspond to $0.05\text{ U}\cdot\text{mL}^{-1}$, $0.1\text{ U}\cdot\text{mL}^{-1}$ and $0.05\text{ mg}\cdot\text{mL}^{-1}$, respectively. UDG excision was carried out with initiator I_U (50 nM) and UDG of varied concentrations in UDG incubation buffer at $37\text{ }^{\circ}\text{C}$ for 15 min.

Supporting Information

For screening UDG inhibitors, 5-FU or gentamycin was introduced into the well-established UDG ($0.05 \text{ U}\cdot\text{mL}^{-1}$) incubation system at $37 \text{ }^\circ\text{C}$ for 15 min, then the incubation mixture was heated up to $95 \text{ }^\circ\text{C}$ for 10 min to deactivate UDG. The subsequent C-HCR readout of the respective fluorescence spectra was carried out in reaction buffer at room temperature ($25 \text{ }^\circ\text{C}$) for a fixed time-interval of 50 min in accordance with the homogeneous UDG assay. The relative activity (RA) of UDG is defined as:

$$\text{RA} = [F_2 - F_0] / [F_1 - F_0]$$

in which F_0 refers to the fluorescence intensity (FAM, $\lambda = 490 \text{ nm}$) of I_U -motivated C-HCR system without UDG whereas F_1 and F_2 are differently defined for the following UDG optimization and inhibition experiments. For optimizing UDG excision temperature, 50 nM I_U was treated with $0.05 \text{ U}\cdot\text{mL}^{-1}$ UDG at different temperature. Then F_1 and F_2 refer to the fluorescence readout (FAM, $\lambda = 490 \text{ nm}$) of the C-HCR-mediated homogeneous UDG assay with an UDG-incubation temperature of $37 \text{ }^\circ\text{C}$ and the corresponding temperature, respectively. For studying gentamycin inhibitory effect, F_1 and F_2 refer to the fluorescence readout (FAM, $\lambda = 490 \text{ nm}$) of the UDG-involved C-HCR system without and with gentamycin, respectively.

Native polyacrylamide gel electrophoresis measurement

For DNA copolymer samples used for gel electrophoresis assay, 20 nM of intact and UDG-treated initiators were incubated with their corresponding hairpin mixtures (H_1+H_2 for HCR-1, $\text{H}_3+\text{H}_4+\text{H}_5+\text{H}_6$ for HCR-2, and $\text{H}_1+\text{H}_2+\text{H}_3+\text{H}_4+\text{H}_5+\text{H}_6$ for C-HCR, the concentrations of all hairpins are the same with that of fluorescence assay) in reaction buffer (10 mM HEPES , 1 M NaCl , 50 mM MgCl_2 , $\text{pH } 7.2$) for 50 min at room temperature ($25 \text{ }^\circ\text{C}$). For gel electrophoresis assay of UDG-involved reaction, unless specified, UDG recognition probes were incubated with UDG in its incubation buffer at $37 \text{ }^\circ\text{C}$ for 15 min to remove uracil groups, and then were treated with NaOH (0.1 M) under $95 \text{ }^\circ\text{C}$ for 10 min. At last, the degraded initiators were neutralized with acetic acid (1 M) and were diluted with Tris-HCl (0.1 M , $\text{pH } 8$) to get a final concentration of 400 nM . Then each of these samples ($10 \text{ } \mu\text{L}$) was mixed with loading buffer and loaded into the notches of the freshly prepared 9% native polyacrylamide gel. Electrophoresis was performed at a constant voltage of 120 V in $1\times\text{TBE}$ buffer (89 mM Tris , 89 mM boric acid , and 2 mM EDTA , $\text{pH } 8.3$) for about 2 h. After electrophoresis, the gel was then stained with $1 \times \text{GelRed}$ and imaged by FluorChem FC3 (ProteinSimple , USA) under UV light (365 nm) irradiation.

Atomic force microscopy (AFM) characterization

For AFM characterization of the C-HCR-motivated branched DNA copolymers and HCR-involved linear nanowires, the C-HCR and HCR samples were respectively prepared in reaction buffer (10 mM HEPES , 1 M NaCl , 50 mM MgCl_2 , $\text{pH } 7.2$) that contained initiator (50 nM) and $\text{H}_1+\text{H}_2+\text{H}_3+\text{H}_4+\text{H}_5+\text{H}_6$ (same condition with the fluorescence assay, for C-HCR) or H_1+H_2 (same condition with the fluorescence assay, for HCR-1). MgCl_2 (5 mM) were deposited on freshly cleaved mica surface ($\text{Structure Probe Inc.}$, USA) for 2 min, followed by their rinsing with ultrapure water and drying under a stream of nitrogen. The DNA sample was diluted and deposited on the mica surface for 15 min to allow its adsorption on the mica surface, followed by its rinsing with water and drying under a stream of nitrogen. The prepared

Supporting Information

sample was scanned under tapping mode by Multimode 8 Atomic Force Microscope with a NanoScope V controller (Bruker Inc.). The silicon tips of AFM analysis were SCANASYST-AIR (tip radius: ~2 nm; resonance frequency: ~70 kHz; spring constant: ~0.4 N/m; length: 115 μm ; width: 25 μm).

Construction of upstream hybridization chain reaction (HCR-1) circuit

As shown in **Figure S1**, the upstream HCR-1 system consists of two hairpins: H_1 and H_2 . H_1 includes the sequence **a-b** that is complementary to initiator **I**. H_2 includes the domain **b-c*** that is complementary to the sequence **c-b*** of hairpin H_1 . H_1 and H_2 is further elongated with the domains **d** and **e** at their 5'- and 3'-ends, respectively. In the presence of initiator **I**, hairpin H_1 opens via a toehold-mediated strand displacement mechanism, leading to the formation of **I- H_1** hybrid. The newly exposed sticky sequence **b*-c** of H_1 opens H_2 via strand displacement mechanism (hybridizing with domain **b-c***), yielding an intermediate structure **I- H_1 - H_2** that includes the same exposed domain **a*-b*** of initiator **I**. This results in an autonomous cross-opening of hairpins H_1 and H_2 and brings the separated segments **d** and **e** into close proximity, leading to the assembly of dsDNA nanowires analogous to alternating copolymers and the concomitant formation of tandem adjacent regions **d** and **e**. Thus **I**-triggered upstream HCR-1 produces chains of the successively reconstituted **d-e** colocalized structure **T**, which then acts as trigger for executing downstream HCR-2.

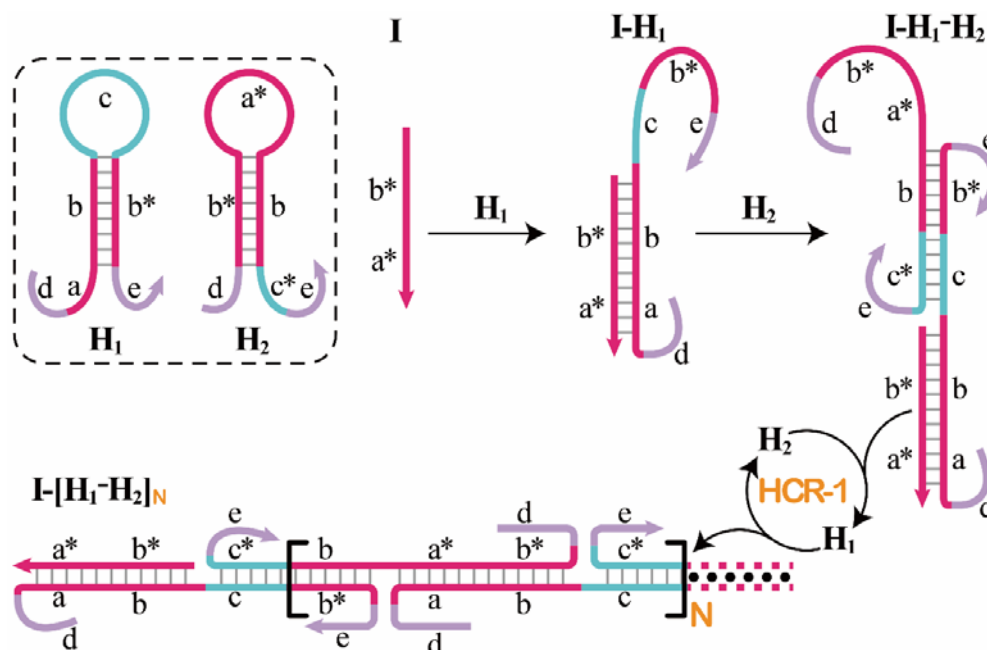


Figure S1. Scheme of the isothermal upstream hybridization chain reaction (HCR-1) circuit.

Construction of downstream hybridization chain reaction (HCR-2) circuit

As shown in **Figure S2**, the downstream HCR-2 system consists of four DNA hairpins: H₃, H₄, H₅ and H₆. H₃ includes the sequence **e*-d*** that can recognize and hybridize with the colocalized structure **T** generated by upstream HCR-1. H₄ includes domain **d*-f*** that is complementary to the sequence **f-d** of hairpin H₃ while H₅ includes domain **g*-d*** that is complementary to the sequence **d-g** of hairpin H₄. H₆ consists of sequence **d*-h*** that is complementary to the sequence **d-g** of hairpin H₄. H₆ also includes sequence **d-e** that is an analog sequence of the colocalized structure **T**. In addition, H₃ is functionalized at its 3'-end with a fluorescence acceptor (TAMRA) while H₅ is functionalized at its 5'-end with a fluorescence donor (FAM). Upon the formation of the tandem repeated structure **T** through the upstream HCR-1 system, segment **e** docks to toehold **e*** of H₃, leading to a toehold-mediated strand displacement reaction which opens TAMRA-labeled H₃ with the formation of an intermediate **T-H₃** structure. And the exposed sequence **d-f** of H₃ hybridizes with H₄, yielding an intermediate structure **T-H₃-H₄**. Then the released single-stranded region **d-g** of H₄ unfolds FAM-labeled H₅, producing an intermediate hybrid **T-H₃-H₄-H₅**. This brings the two fluorophores (FAM and TAMRA) into close proximity and enables the Förster resonance energy transfer (FRET) process. The single-stranded sequence **h-d** of H₅ again unlocks H₆, of which the sequestered sequence **d-e** gets exposed and leads to HCR-2-involved multiple assembly of H₃, H₄, H₅ and H₆ into long dsDNA copolymers.

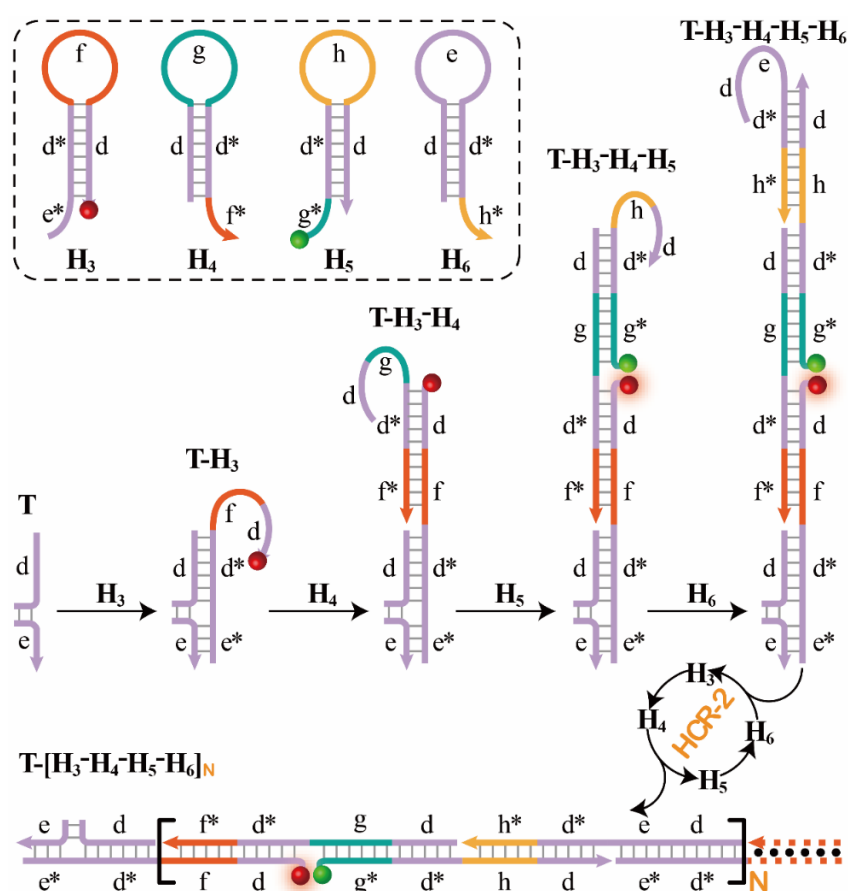


Figure S2. Scheme of the downstream hybridization chain reaction (HCR-2) circuit.

Optimization of the C-HCR system

The initial concentrations of hairpins are as follows: H₁ 100 nM, H₂ 100 nM, H₃ 200 nM, H₄ 100 nM, H₅ 100 nM, H₆ 100 nM, and the concentrations of labeled H₃ and H₅ are kept constant for getting better FRET performance. To improve the signal-to-background ratio of the C-HCR system, the concentration effects of hairpins were extensively investigated. No fluorescence change was observed upon increasing the concentrations of H₁, H₂, H₄ and H₆, indicating the metastable characteristic of C-HCR circuit without signal leakage. Comparing with the initial working conditions of C-HCR (bar chart a, **Figure S3**), no significant improvement of fluorescence response could be observed by doubling the concentrations of H₄ and H₆ (bar chart b, **Figure S3**), a slightly increased fluorescence response was revealed by doubling the concentrations of H₂, H₄ and H₆ (bar chart c, **Figure S3**), whereas a significantly amplified fluorescence response was obtained by doubling the concentrations of H₁, H₄ and H₆ (bar chart d, **Figure S3**). It is clear that the colocalized structure **T** of H₁-involved HCR-1 triggers HCR-2 more effectively than that of H₂-involved HCR-1, which is consistent with the fluorescence experiments of **Figure S4C** and **S4D** where the H_{2T}-substituted HCR system shows a better amplification performance than that of the H_{1T}-substituted HCR system. This might be attributed to the different microenvironment of the corresponding colocalized structure **T**. The optimized concentrations are then adapted in the subsequent experiments and fixed as follows: 200 nM H₁, 100 nM H₂, 200 nM H₃, 200 nM H₄, 100 nM H₅ and 200 nM H₆.

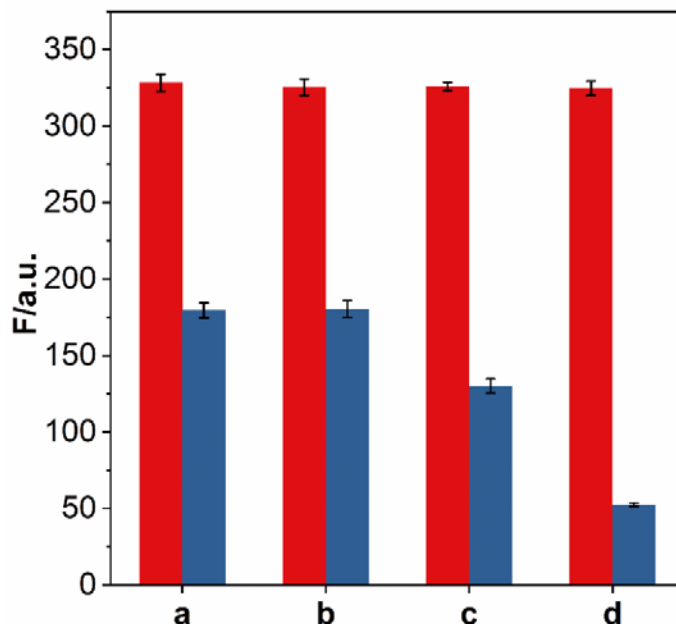


Figure S3. Fluorescence changes (at $\lambda = 520$ nm) of the C-HCR mixture containing 100 nM H₁, 100 nM H₂, 200 nM H₃, 100 nM H₄, 100 nM H₅, and 100 nM H₆ (a) and upon doubling the concentrations of H₄ and H₆ (b), H₂, H₄ and H₆ (c), and H₁, H₄ and H₆ (d) of state a. The red and blue bars show the fluorescence intensities of C-HCR system without and with 50 nM initiator, respectively. Error bars were derived from n = 5 experiments.

Demonstration of C-HCR strategy

To implement C-HCR circuit, both of HCR-1 and HCR-2 are indispensable as revealed by control experiments, where one of the non-fluorescent hairpin components (H_1 , H_2 , H_4 , or H_6) was removed or substituted from the C-HCR mixture. As shown in **Figure S4A** and **S4B**, scarcely no fluorescence changes were observed for initiator-motivated C-HCR by subtracting hairpin H_1 or H_2 from upstream HCR-1 (points a and b, **Figure S4A**) or by subtracting hairpin H_4 from downstream HCR-2 (point c, **Figure S4A**). However, an inapparent fluorescence change was observed for triggered C-HCR mixture without H_6 (point d, **Figure S4A**). It is reasonable since upstream HCR-1 was totally blocked without hairpin H_1 or H_2 while downstream HCR-2 and C-HCR was significantly blocked without hairpin H_4 . In addition, the H_6 -expelled C-HCR corresponds to a conventional HCR system where the intact HCR-1 executes a well-established single-stage amplification while the subsequent H_6 -excluded HCR-2 executes a simple signal readout function. Evidently, C-HCR is only activated with both upstream HCR-1- and downstream HCR-2-involved reactants. Moreover, the non-fluorescent hairpin components (H_1 and H_2) were substituted to further probe the underlying working principle where H_1 and H_2 were respectively converted to H_{1T} and H_{2T} once the constitute domains e and g were replaced with poly(T) sequences. Accordingly, the autonomous H_{1T} - H_{2T} cross-hybridization cannot produce triggers for downstream HCR-2 while each H_1 - H_{2T} or H_{1T} - H_2 pair hybridization event produces only one trigger for generating HCR-2 copolymeric dsDNA nanowires (**Figure S4C** and **S4D**). As expected, no fluorescence change was observed for $H_{1T}+H_{2T}+H_3+H_4+H_5+H_6$ mixture as the output of HCR-1 could not transduce into HCR-2 circuit, point a of **Figure S4D**. Meanwhile, a moderate fluorescence change was observed for $H_{1T}+H_2+H_3+H_4+H_5+H_6$ or $H_1+H_{2T}+H_3+H_4+H_5+H_6$ mixture, points b and c of **Figure S4D**, respectively. Albeit the fluorescence change is higher than that of the H_6 -excluded C-HCR system, it is still much lower (only 25%~50%) than that of original C-HCR system, point d, **Figure S4D**. Obviously, the C-HCR-motivated successive cross-opening of the hairpin reactants leads to an effectively amplified FRET generation. All of these results could be easily explicated as follows. Target signaling occurs in linear amplification with a multiple reaction ratio (1:N) in conventional HCR (H_6 -expelled C-HCR), whereas one target yields quadratic signal amplification ($1:N^2$) in the H_{1T} - or H_{2T} -replaced C-HCR system, and one target generates doubled quadratic signal amplification ($1:2N^2$) in the present C-HCR. The theoretical analysis shows a good agreement with the fluorescence measurements, which facilitates the amplified detection of trace amount of targets through the current C-HCR amplifier.

Supporting Information

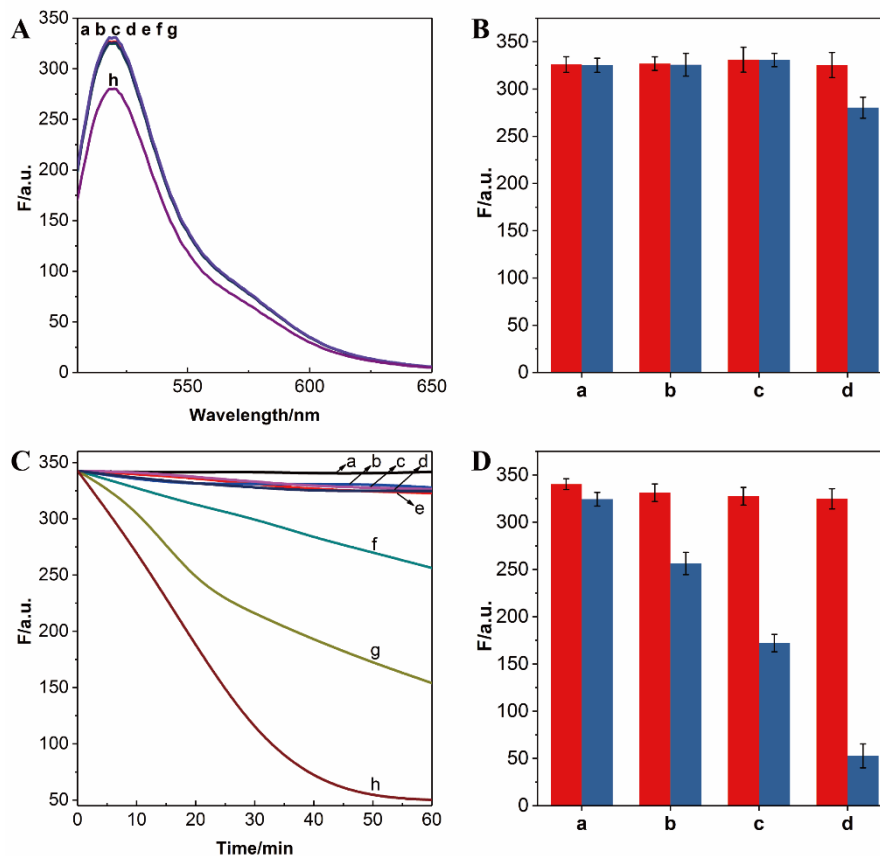


Figure S4. (A) Fluorescence spectra generated by the C-HCR system without hairpin H₁ (a. 50 nM initiator, e. no initiator), H₂ (b. 50 nM initiator, f. no initiator), H₄ (c. 50 nM initiator, g. no initiator), or H₆ (d. 50 nM initiator, h. no initiator). (B) Fluorescence changes (at $\lambda=520$ nm) of the C-HCR mixture upon subtracting H₁ (a), H₂ (b), H₄ (c) or H₆ (d) from the system. (C) Time-dependent fluorescence changes of intact C-HCR circuit (d. no initiator, h. 50 nM initiator) and upon replacing H₁ with H_{1T} (b. no initiator, f. 50 nM initiator), H₂ with H_{2T} (c. no initiator, g. 50 nM initiator), and H₁ and H₂ with H_{1T} and H_{2T} (a. no initiator, e. 50 nM initiator) from the C-HCR system. (D) Fluorescence changes (at $\lambda=520$ nm) of the C-HCR mixture upon replacing H₁ with H_{1T} (b), H₂ with H_{2T} (c), H₁ and H₂ with H_{1T} and H_{2T} (a), and none of the hairpins (d) from the system. The red and blue bars show the fluorescence intensities of the C-HCR system without and with 50 nM initiator, respectively. Error bars were derived from $n = 5$ experiments.

Gel electrophoresis characterization of C-HCR system

Gel electrophoresis was carried out to verify upstream HCR-1, downstream HCR-2 and the integrated C-HCR circuits, **Figure S5**. No new band emerged for HCR-1, HCR-2 and C-HCR reactants in the absence of their corresponding triggers, indicating the hairpins mixtures are metastable without initiators. Many new bright bands with a maximum size of thousands of base-pairs were obtained while the bands of monomer hairpins became weakened for the respective triggered HCR-1, HCR-2 and C-HCR systems. It is clear that HCR-1, HCR-2 or cascaded HCR-1/HCR-2 (C-HCR) can only be triggered by their corresponding initiators, yielding high-molecular-weight dsDNA copolymeric nanostructures composed of hundreds of the respective hairpin components, which is consistent with those of fluorescence experiments shown in **Figure 1B** and **1C**.

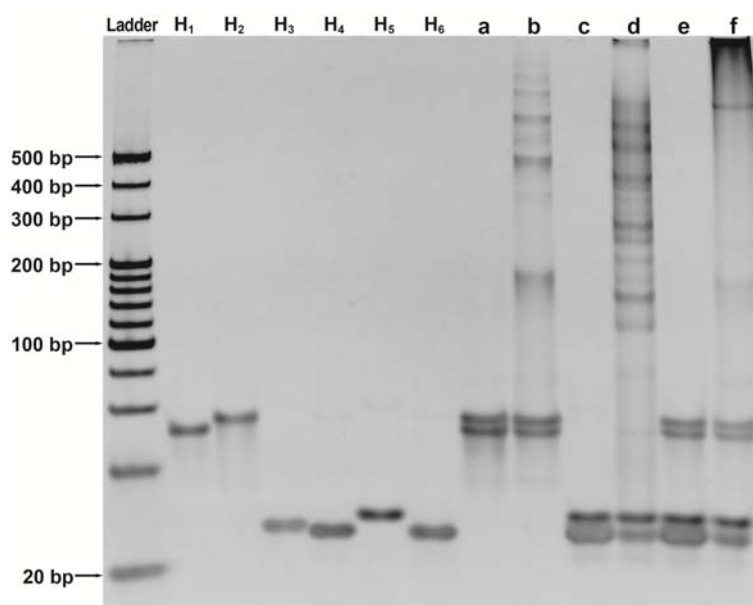


Figure S5. Native gel electrophoresis of C-HCR and its individual upstream HCR-1 and downstream HCR-2 constituents. (a) H₁ + H₂ mixture; (b) H₁ + H₂ mixture and its initiator; (c) H₃ + H₄ + H₅ + H₆ mixture; (d) H₃ + H₄ + H₅ + H₆ mixture and its initiator; (e) H₁ + H₂ + H₃ + H₄ + H₅ + H₆ mixture; (f) H₁ + H₂ + H₃ + H₄ + H₅ + H₆ mixture and its initiator.

AFM investigation of C-HCR circuit

The structural characteristics of C-HCR-generated DNA nanostructures were further studied by atomic force microscopy (AFM). Only tiny spots of the C-HCR hairpin monomers without any assembled product were observed for non-triggered C-HCR without initiator (**Figure S6A**) while long branched DNA polymeric nanowires were observed for target-triggered C-HCR (**Figure S6B**). The height of the DNA nanostructures was measured to be ~ 1.5 nm (**Figure S6D**), which corresponds to a characteristic dsDNA. It is reasonable since downstream HCR-2 nucleates and produces copolymeric dsDNA nanowires from each of the tandem colocalized triggers of upstream HCR-1 nanowires, leading to the formation of branched dsDNA nanowires. As an important control, AFM imaging of the target-triggered HCR-1 shows a long linear DNA structure (**Figure S6C**), validating the robustness of our C-HCR system. In conclusion, these results clearly demonstrate the successful implementation and the significant signal amplification capacity of our C-HCR circuit.

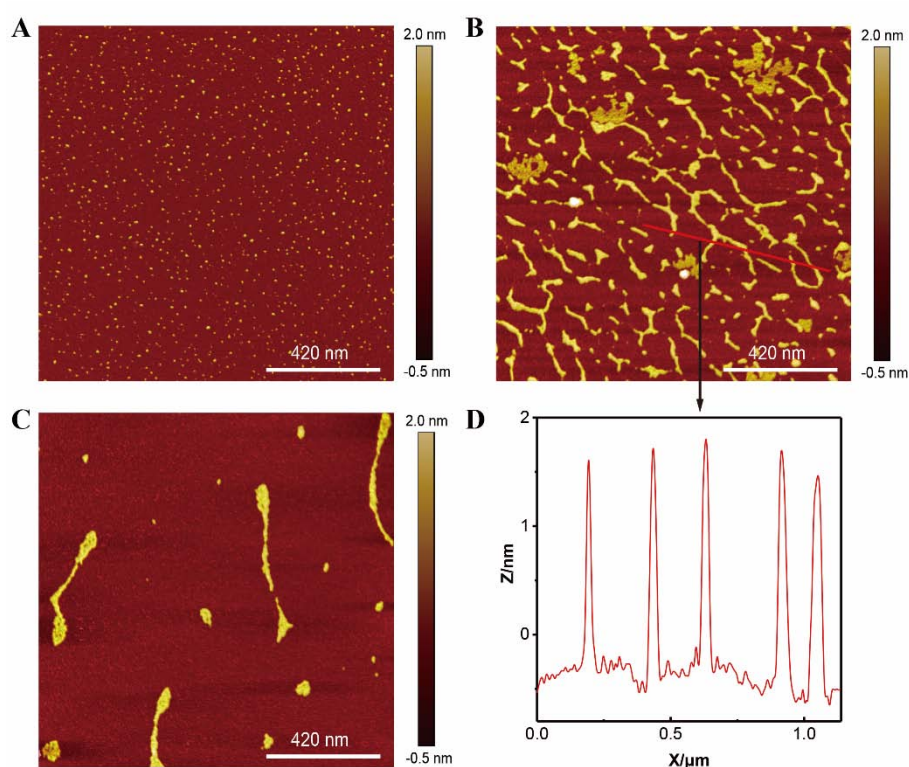


Figure S6. (A) AFM image of C-HCR mixture without initiator. (B) AFM image of C-HCR product. (C) AFM image of HCR-1 product. Detailed experiment conditions are shown in experimental section. (D) Height profiles of the C-HCR-generated branched dsDNA nanowires as probed by AFM cross-section analysis. The C-HCR sample was prepared in reaction buffer (10 mM HEPES, 1 M NaCl, 50 mM MgCl₂, pH 7.2) that contained 200 nM H₁, 100 nM H₂, 200 nM H₃, 200 nM H₄, 100 nM H₅, 200 nM H₆ and 50 nM initiator. Detailed experiment conditions are shown in experimental section.

Investigation of the specific UDG-substrate interactions

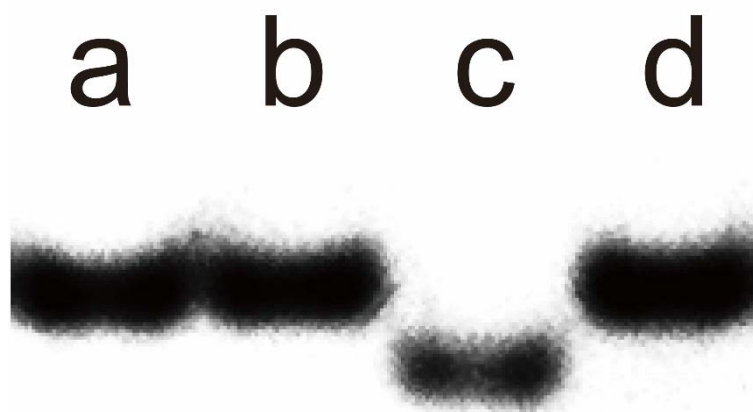


Figure S7. Native gel electrophoresis verifications of the specific recognition of UDG with its substrate: (a) UDG-recognition initiator I_U , (b) normal initiator I , (c) UDG-recognition initiator I_U treated with $0.5 \text{ U}\cdot\text{mL}^{-1}$ UDG, and (d) normal initiator I treated with $0.5 \text{ U}\cdot\text{mL}^{-1}$ UDG. These probes were incubated with UDG in its incubation buffer at $37 \text{ }^\circ\text{C}$ for 15 min, and then were treated with NaOH (0.1 M) under $95 \text{ }^\circ\text{C}$ for 10 min. At last, these UDG-treated initiators were neutralized with acetic acid (1 M) and were diluted with Tris-HCl (0.1 M, pH 8) for gel electrophoresis measurement.

Optimization of UDG recognition probe

To achieve a robust UDG sensing platform of higher performance, the UDG recognition probe I_U needs to be further optimized to improve the signal-to-background ratio of C-HCR amplifier. The fluorescence changes ($\Delta F = F - F_0$) of different abasic UDG recognition probes were utilized to evaluate and optimize the different performance of the C-HCR-mediated homogeneous UDG assay (**Figure S8**). The respective thymine bases of toehold and branch migration domains were substituted with uracil groups to generate the corresponding toehold- and migration-specific UDG recognition probes I_{UT} and I_{UM} . Interestingly, the toehold-specific UDG probe I_{UT} shows a better UDG-sensing performance, which is presumably attributed to the dominating toehold-mediated strand displacement of the present C-HCR process. Furthermore, the number of substituted uracil groups also plays an important role for amplified UDG assay, and the two-uracil-containing toehold-specific UDG recognition probe I_U shows the best performance. This might originate from a much lower binding affinity of the degraded I_U probe with more AP sites, which generate a much distinct signal for homogeneous UDG assay.

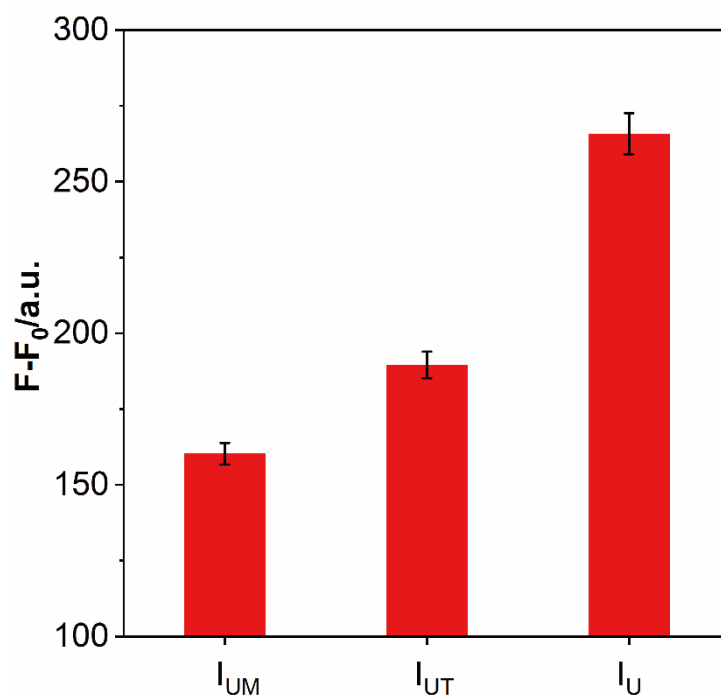


Figure S8. Optimization of UDG recognition probe as revealed by fluorescence measurements. Fluorescence changes (at $\lambda = 520$ nm) of C-HCR-based UDG sensing platform triggered with different UDG-treated recognition probes for 50 min. $0.5 \text{ U} \cdot \text{mL}^{-1}$ UDG-involved excision was carried out in UDG incubation buffer (20 mM Tris-HCl, 1 mM DTT, 1 mM EDTA, pH 8) containing the respective UDG probes at 37°C for 15 min. Error bars were derived from $n = 5$ experiments.

Optimization of UDG-involved reaction conditions

The UDG-involved excision time was studied by incubating a fixed amount of UDG with the optimized recognition probe I_U for varied reaction time. Then the abasic I_U probe was introduced into the present C-HCR system, **Figure S9A**. The fluorescence intensity of FAM increased gradually with prolonged enzymatic reaction time under 37 °C, and finally reached a plateau after an incubation time of 15 min. The UDG-motivated degradation of I_U probe turned out to dominate the prohibition of C-HCR amplifier and FRET signal generation, making the intensified fluorescence of FAM with increasing reaction time. The result suggested that I_U probe was increasingly recognized and cleaved with prolonged enzymatic incubation time until the reaction time reaches 15 min when all of I_U probe was completely degraded. Thus a fixed incubation time of 15 min was then applied as the optimized reaction time for the subsequent experiments. The environmental temperature also plays an important role for achieving an effective UDG-mediated biotransformation. Then the effect of reaction temperature was studied by incubating a fixed concentration of UDG with the optimized probe I_U for an optimized time-interval of 15 min under the different temperatures. It is clear that an incubation temperature of 37 °C shows the best performance for the homogeneous UDG assay (**Figure S9B**), which is consistent with the official instruction of the UDG enzyme. Accordingly, 37 °C was chosen as the optimized incubation condition for the following experiments.

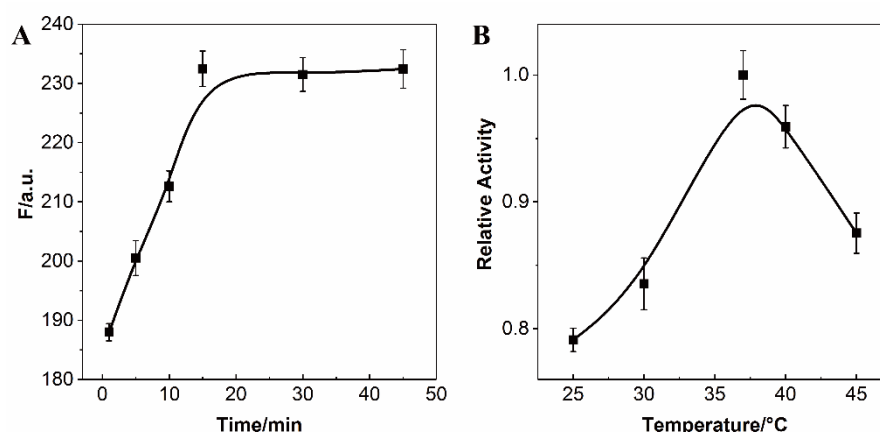


Figure S9 (A) Optimization of UDG-incubation time as revealed by fluorescence measurement. Fluorescence changes (at $\lambda = 520$ nm) of C-HCR-based homogeneous UDG sensing platform with different enzymatic reaction time at 37 °C. $0.05 \text{ U} \cdot \text{mL}^{-1}$ UDG-involved excision was carried out in UDG incubation buffer (20 mM Tris-HCl, 1 mM DTT, 1 mM EDTA, pH 8) at -37 °C. (B) Optimization of UDG-incubation temperature as revealed by fluorescence measurements. $0.05 \text{ U} \cdot \text{mL}^{-1}$ UDG excision was carried out in UDG incubation buffer at varied temperature for 15 min. The C-HCR readout system consisting of 200 nM H_1 , 100 nM H_2 , 200 nM H_3 , 200 nM H_4 , 100 nM H_5 and 200 nM H_6 was carried out in reaction buffer (10 mM HEPES, 1 M NaCl, 50 mM MgCl_2 , pH 7.2) for a fixed time-interval of 50 min. Error bars were derived from $n = 5$ experiments.

Traditional HCR-1-mediated UDG assay

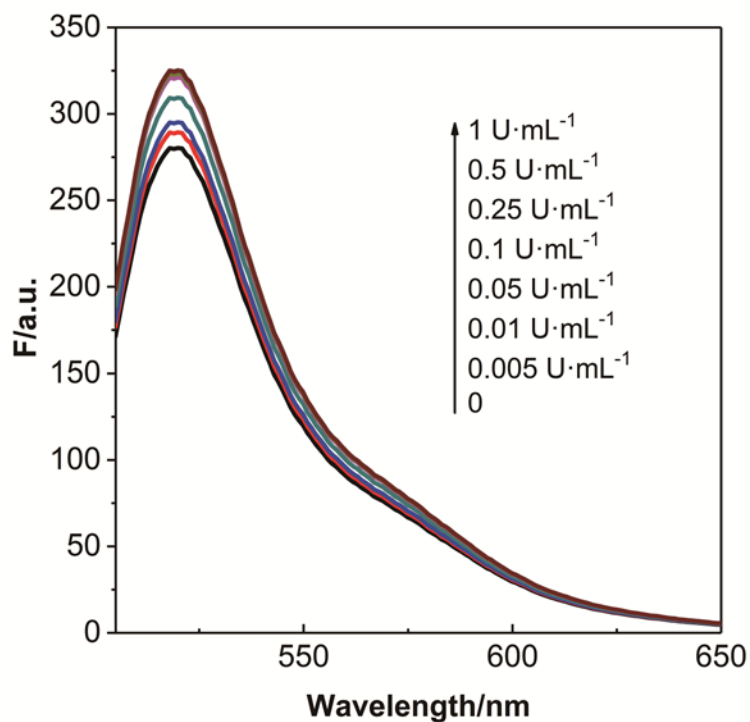


Figure S10. Fluorescence spectra generated by the traditional HCR-1 system with different concentrations of UDG. UDG excision was carried out with 50 nM initiator I_U and varied concentrations of UDG in incubation buffer (20 mM Tris-HCl, 1 mM DTT, 1 mM EDTA, pH 8) at 37 °C for 15 min. The traditional HCR-1 system consisting of 200 nM H_1 , 100 nM H_2 , 200 nM H_3 , 200 nM H_4 and 100 nM H_5 was carried out in reaction buffer (10 mM HEPES, 1 M NaCl, 50 mM $MgCl_2$, pH 7.2) for a fixed time interval of 50 min.

The kinetics analysis of the specific UDG-substrate interactions

The relationship between the initial catalytic rate and substrate concentration was studied, **Figure S11**. V_0 is the initial UDG excise rate represented in consumed substrate I_U per second while $[S]$ is the concentration of probe I_U represented in μM . Plotting $1/V_0$ versus $1/[S]$ yields the Lineweaver–Burk plot. An obvious linear profile of the plot indicates that the kinetics data fits well with the Michaelis–Menten equation. Then the important kinetic parameters, K_M and k_{cat} , are calculated by the equation to be $1.53 \mu\text{M}$ and 4.37 s^{-1} , respectively, which are close to the previous reports,¹⁻² suggesting that the present C-HCR-amplifier could be adapted as a convenient and versatile tool for probing the detailed reaction process of various biotransformations. The varied parameters might be attributed to the different conditions (including structure variations of UDG substrates and molecular probes) and sensing platforms.

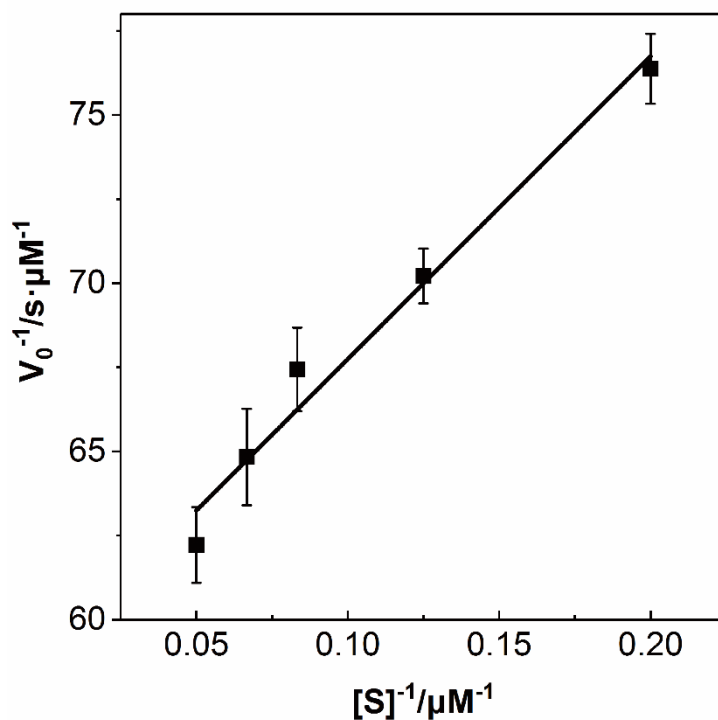


Figure S11. Lineweaver–Burk plot of UDG-catalyzed uracil removal as studied by C-HCR-amplified sensing platform. UDG excision was carried out with $0.05 \text{ U}\cdot\text{mL}^{-1}$ UDG and varied concentrations of initiator I_U in UDG incubation buffer (20 mM Tris-HCl, 1 mM DTT, 1 mM EDTA, pH 8) at $37 \text{ }^\circ\text{C}$ for 30 s. The C-HCR system consisting of 200 nM H_1 , 100 nM H_2 , 200 nM H_3 , 200 nM H_4 , 100 nM H_5 and 200 nM H_6 was carried out in reaction buffer (10 mM HEPES, 1 M NaCl, 50 mM MgCl_2 , pH 7.2) for a fixed time interval of 50 min. Error bars were derived from $n = 5$ experiments.

Supporting Information

Table S1. The DNA sequences used to construct the amplified sensing platform

No.	Sequence (5'→3')
H₁	GCTTCATCTTCATCTCTAATTCGGAGCTAGGTAG GTAGAGATATGCCGTCTACCTACCTAGCTCCGACTC
H₂	GCTTCATCTTCATCTCCGTCTACCTACCTAGCTCC GAATTAGAGCTAGGTAGGTAGACGGCATATCACACTC
H₃	GAGTGTCCGAGATGAAGATGAAGC CATCGTGCTTCATCTTCATCTCCG (TAMRA)
H₄	GCTTCATCTTCATCTCCGGTTTT GCCGAGATGAAGATGAAGCACGATG
H₅	(FAM) CAAAACCGGAGATGAAGATG AAGCTTGCCTGCTTCATCTTCATCTCCG
H₆	GCTTCATCTTCATCTCCGACTCC GGAGATGAAGATGAAGCAGGCAA
H_{1T}	TTTTTTTTTTTTTTTTCTAATTCGGAGCTAGGTAG GTAGAGATATGCCGTCTACCTACCTAGCTCCGTTTTTT
H_{2T}	TTTTTTTTTTTTTTTTCCGTCTACCTACCTAGCTCC GAATTAGAGCTAGGTAGGTAGACGGCATATCTTTTTT
I	TCTACCTACCTAGCTCCGAATTAG
T	GCTTCATCTTCATCTCCGACTC
I_U	TCTACCTACCTAGCTCCGAA <u>UU</u> AG
I_{UT}	TCTACCTACCTAGCTCCGAAT <u>U</u> AG
I_{UM}	TCTACC <u>U</u> ACCTAGCTCCGAATTAG

Supporting Information

Table S2. Summary of the present amplification methods for UDG assay

Methods	Analytical time (min)	Linear range (U·mL ⁻¹)	Detection limit (U·mL ⁻¹)	Ref.
Colorimetric assay based on UDG-mediated activation of G-quadruplex	95	0.008-0.2	0.008	3
Fluorescence assay based on UDG-triggered formation of G-quadruplex	165	0-0.05	0.00044	4
Fluorescence assay based on UDG-mediated deactivation or activation of DNazymes	14	0-0.27	0.0034	5
SERS assay based on UDG-mediated FAM dye approaching to Ag nanorods surface	65	0.003-0.5	0.003	6
Electrochemical assay based on UDG-induced strand displacement	180	0.025-2	0.012	7
Fluorescence polarization detection of UDG based on Tungsten disulfide nanosheet and exonuclease III-assisted signal amplification	100	0.0008-0.4	0.0003	8
Fluorescence assay based on RCA-mediated DNazyme amplification	390	0-1	0.002	9
Fluorescence UDG assay based on exonuclease I-involved signal amplification	20	0.01-5	0.007	10
Fluorescence assay based on traditional HCR-mediated UDG assay	65	0-0.01	0.0013	This work
Fluorescence assay based on C-HCR-amplified UDG assay	65	0-0.005	0.00011	This work

References

- 1 G. Slupphaug, C. D. Mol, B. Kavli, A. S. Arvai, H. E. Krokan and J. A. Tainer, *Nature* 1996, **384**, 87-92.
- 2 E. Seibert, J. B. A. Ross and R. Osman, *Biochemistry* 2002, **41**, 10976-10984.
- 3 H. Nie, W. Wang, W. Li, Z. Nie and S. Yao, *Analyst* 2015, **140**, 2771-2777.
- 4 Y. Wu, L. Wang, J. Zhu and W. Jiang, *Biosens. Bioelectron.*, 2015, **68**, 654-659.
- 5 X. Yu and L. Yi, *Anal. Chem.*, 2012, **84**, 9981-9987.
- 6 Y. Huang, S. Liao, M. Xiong, Y. Ma, J. Zhao and S. Zhao, *Anal. Methods* 2016, **9**, 786-791.
- 7 X. Liu, M. Chen, T. Hou, X. Wang, S. Liu and F. Li, *Electrochim. Acta* 2013, **113**, 514-518.
- 8 J. Zhao, Y. Ma, R. Kong, L. Zhang, W. Yang and S. Zhao, *Anal. Chim. Acta* 2015, **887**, 216-223.
- 9 L. Zhang, J. Zhao, J. Jiang and R. Yu, *Chem. Commun.*, 2012, **48**, 8820-8822.
- 10 Y. Ma, J. Zhao, X. Li, L. Zhang and S. Zhao, *RSC Adv.*, 2015, **5**, 80871-80874.